Individualized Prediction of Early Alzheimer's Disease Based on Magnetic Resonance Imaging Radiomics, Clinical, and Laboratory Examinations: A 60-Month Follow-Up Study

Lin Tang, MM,[1†] Xiaojia Wu, MM,[1†] Huan Liu, MD,[2] Faqi Wu, MM,[3] Rao Song, MM,[1] Wei Zhang, MD,[1] Dajing Guo, MD,[1] Junbang Feng, MM,[4] and Chuanming Li, MD[1*]

Background: Accurately predicting whether and when mild cognitive impairment (MCI) will progress to Alzheimer's disease (AD) is of vital importance to help developing individualized treatment plans to defer the occurrence of irreversible dementia.

Purpose: To develop and validate radiomics models and multipredictor nomogram for predicting the time to progression (TTP) from MCI to AD.

Study Type: Retrospective.

Population: One hundred sixty-two MCI patients (96 men and 66 women [median age, 72; age range, 56–88 years]) were included from the Alzheimer's Disease Neuroimaging Initiative (ADNI) database.

Field Strength/Sequence: T_1-weighted imaging and T_2-weighted fluid-attenuation inversion recovery imaging acquired at 3.0 T.

Assessment: During the 5-year follow-up, 68 patients converted to AD and 94 remained stable. Patients were randomly divided into the training ($n = 112$) and validation datasets ($n = 50$). Radiomic features were extracted from the whole cerebral cortex and subcortical nucleus of MR images. A radiomics model was established using least absolute shrinkage and selection operator (LASSO) Cox regression. The clinical-laboratory model and radiomics-clinical-laboratory model were developed by multivariate Cox proportional hazard model. The performance of each model was assessed by the concordance index (C-index). A multipredictor nomogram derived from the radiomics-clinical-laboratory model was constructed for individualized TTP estimation.

Statistical Tests: LASSO cox regression, univariate and multivariate Cox regression, Kaplan–Meier analysis and Student's t test were performed.

Results: The C-index of the radiomics, clinical-laboratory and radiomics-clinical-laboratory models were 0.924 (95% confidence interval [CI]: 0.894–0.952), 0.903 (0.868–0.938), 0.950 (0.929–0.971) in the training cohort and 0.811 (0.707–0.914), 0.901 (0824–0.977), 0.907 (0.836–0.979) in the validation cohort, respectively. A multipredictor nomogram with 15 predictors was established, which had high accuracy for individual TTP prediction with the C-index of 0.950 (0.929–0.971).

Data Conclusion: The prediction of individual TTP from MCI to AD could be accurately conducted using the radiomics-clinical-laboratory model and multipredictor nomogram.

Evidence Level: 3

Technical Efficacy: 2

Alzheimer's disease (AD) is characterized by cognitive and behavioral deficits and is regarded as one of the most common progressive and irreversible neurodegenerative diseases.[1] In 2018, approximately 50 million people worldwide suffered from dementia, which will triple by 2050.[2] AD not only has an impact on a patient's daily life but also has a serious impact on the psychological and economic status of their family.[1] Until now, no breakthrough in the direct treatment of AD has been achieved. However, studies have shown that intervention in the early stage of AD may delay the occurrence of irreversible dementia.[3] Mild cognitive impairment (MCI) is generally defined as a transition stage between normal cognition and AD,[4] with approximately 10%–20% of patients converting to dementia annually.[5] Therefore, it is of vital importance to accurately predict whether and when MCI will progress to AD, then develop personalized follow-up plans, and perform a timely intervention to delay the progression of AD.

Many of the previous studies considered the prediction of AD by MCI as a binary classification task.[6–8] In accordance with the results of follow-up, MCI subjects were divided into progressive MCI (pMCI) and stable MCI (sMCI) subjects.[9] Binary classifiers could be trained on a basis of baseline data to distinguish between patient groups. This prediction method is unable to provide specific information regarding when MCI patients would cross the threshold and enter AD. Recent studies have shifted the focus to predict the progression of AD during follow-up using time-to-event analysis techniques.[10–12] However, most existing studies have used relatively simple and large-scale imaging indicators, including cerebral volume, cortical thickness, and geometric features of the hippocampus and temporal lobe cortex.[10–12] The roles of white matter and subcortical nucleus have been mostly ignored. In fact, structural changes in the basal ganglia and thalamus have been identified as risk factors for MCI transformation.[13–15] Compared with sMCI, pMCI showed more severe amygdala atrophy.[14] The severity of white matter lesions is also associated with cognitive decline.[16] On the other hand, unlike large-scale indicators of brain atrophy, subtle changes caused by the accumulation of amyloid β (Aβ) and tau proteins before atrophy are more early changes, which cannot be detected by conventional MRI techniques and naked eye observation.[17] Radiomics is a new technology that can be used to extract a large number of quantitative features from medical images with automatic high throughput, with subsequent data mining.[18] And radiomic features usually could be divided into four categories: intensity, shape, texture (gray-level co-occurrence matrix [GLCM], gray-level run-length matrix [GLRLM], and gray-level size zone matrix [GLSZM]), and wavelet texture. It has been successfully applied to provide accurate diagnosis and evaluation of tumors,[19] psychiatric disorders,[20] and neurodegenerative diseases.[21]

The risk of MCI progression increased rapidly with the extension of follow-up time. About 60% of MCI patients conversion could be detected at 3-year follow-up, and this proportion would increase to 80% at 4-year follow-up.[22,23] Previous studies usually focused on the progression of MCI within 12–36 months,[24–26] which might ignore the transformed patients after the third year. It is of necessity to extend the follow-up time to improve the stability and accuracy of the prognosis. Therefore, this study aimed to establish and validate a radiomics model, which extracted features from the whole brain microstructure and combined with clinical and laboratory characteristics to accurately predict the progression time of MCI patients in 5 years.

Materials and Methods

Participants

Data used in the preparation of this study were obtained from the Alzheimer's Disease Neuroimaging Initiative (ADNI) database (adni. loni.usc.edu). The ADNI study was approved by an ethics standards committee on human experimentation at each institution. Written informed consent was obtained from all participants. In total, data from 162 MCI patients were obtained from the ADNI database, including the ADNI-GO and ADNI-2. All patients had T_1-weighted imaging (T_1WI), T_2-weighted fluid-attenuated inversion recovery (T_2-FLAIR) imaging and complete clinical and laboratory characteristics at the baseline of data collection. Among them, 68 pMCI patients were diagnosed with AD in a period of time (range 6–60 months, the follow-up interval was 6–12 months during the first 3 years, and 12 months during the 3–5 year), 94 sMCI patients were not converted to AD during the 5-year follow-up. The diagnosis of AD was made according to the criteria made by the National Institute of Neurological and Communicative Disorders and Stroke and Alzheimer's disease and Related Disorders Association. Participants who were diagnosed with bidirectional changes (MCI to AD, and back to MCI) during the follow-up period were excluded. All MCI patients were randomly divided into the training cohort ($n = 112$) and validation cohort ($n = 50$) with a rate of 7:3. Figure 1 shows the working flow of this study.

Clinical and Laboratory Characteristics

Clinical and laboratory characteristics were directly collected from the ADNI website. The demographic information included age, sex, education level, body mass index (BMI), and alcohol use. Twelve neuropsychological scales were used to characterize the cognitive function at baseline, containing the Montreal Cognitive Assessment (MOCA), the Alzheimer's Disease Assessment Scale (ADAS, both 13 and 11 questionnaires), the Clinical Dementia Rating (CDR), the Functional Activities Questionnaire (FAQ), the Geriatric Depression Scale (GDS), the Mini-Mental State Examination (MMSE), the Rey Auditory-Verbal Learning Test (RAVLT: RAVLT immediate, RAVLT learning, RAVLT forgetting, RAVLT percent forgetting), and the Animal Fluency Test (AFT).[9,12,22,23,27,28] Laboratory characteristics included the cerebrospinal fluid (CSF) amyloid-beta peptides (Aβ, both Aβ1-42, Aβ1-40, and Aβ1-38),
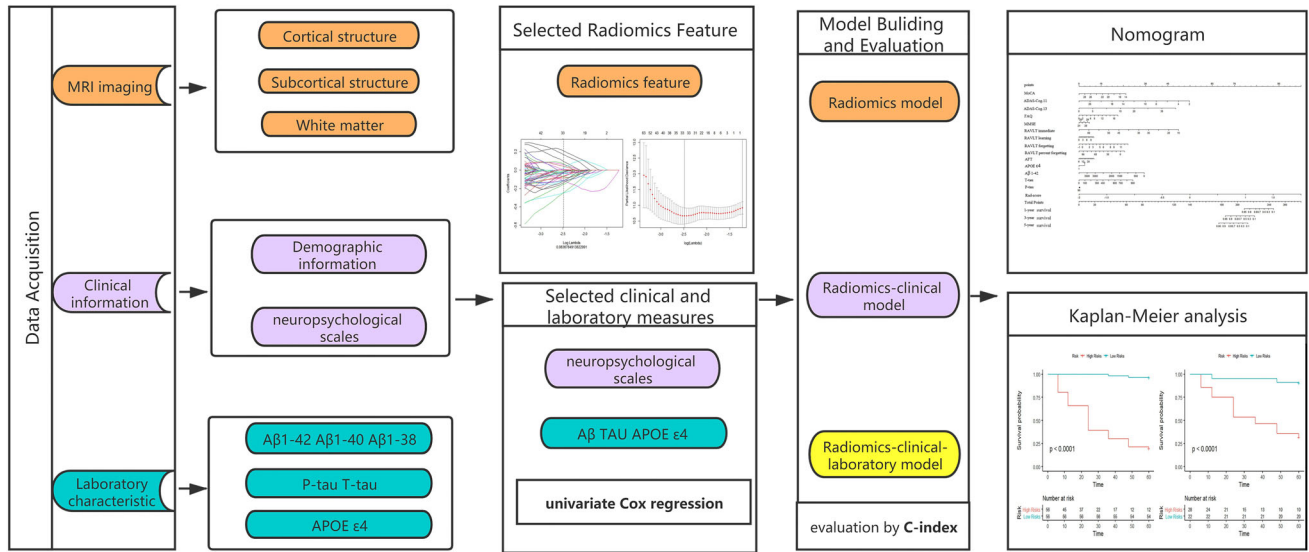
FIGURE 1: The working flow chart of this study.

phosphorylated tau (P-tau), total tau (T-tau), and APOE ε4. Clinical variables and laboratory characteristics are summarized in Table 1.

MRI Acquisition and Radiomics Features Extraction

For all subjects, standard T1-weighted anatomical imaging was performed by volumetric three-dimensional magnetization-prepared rapid gradient-echo (3D-MPRAGE) or equivalent scheme with slightly different resolutions among patients. Detailed imaging parameters were provided at ADNI website. The MR images acquired using scanner 1 (Siemens Medical Solutions) were scanned with the parameters as follows: (repetition time [TR]/echo time [TE] = 2300.0/3.0 msec, matrix = 240 × 256 × 176). The MR images acquired using scanner 2 (General Electric Healthcare) were scanned with the parameters as follows: TR/TE = 7.7–7.0/3.1–2.8 msec, matrix = 256 × 256 × 196. The MR images acquired using scanner 3 (Philips Medical Systems) were scanned with the parameters as follows: TR/TE = 6.8/3.1 msec, matrix = 256 × 256 × 170. More detailed information about the image acquisition procedures is available on the ADNI website. (http://adni.loni.usc.edu/methods/documents/).

FreeSurfer (v6.0.0) (https://surfer.nmr.mgh.harvard.edu/) was used for feature extraction of the cortex. Preprocessing involved the following steps: motion correction, skull stripping, coordinate transformation, gray–white matter segmentation, reconstruction of cortical surface models, region labeling, registration, and statistical analysis. The whole cortex was divided by the Destrieux atlas.[29] The cortex indicators, including surface area, average thickness, standard deviation of thickness, integrated rectified Gaussian curvature, integrated rectified mean curvature, intrinsic curvature index, folding index, and gray matter volume, were obtained from each of the brain regions.

The Statistical parametric mapping 12 (Wellcome Department of Cognitive Neurology, UCL, London, UK) and Brainnetome fMRI Toolkit (http://brant.brainnetome.org) were used for the subcortical brain region segmentation. First, the T_1-weighted images were converted to Neuroimaging Informatics Technology Initiative (NIFTI) data. Then, images were normalized to the Montreal Neurological Institute (MNI) standard T1 template (standard space 181 × 217 × 181 with a resolution of 1 mm × 1 mm × 1 mm). Meanwhile, this study resliced the Brainnetome Atlas to the standard MNI space with a resolution of 1 mm × 1 mm × 1 mm. Bilateral hippocampus and 12 subcortical nuclei including the thalamus, putamen, globus pallidus, caudate nucleus, nucleus accumbens, and amygdala were further extracted as masks. Finally, for each subject, the volumes of interests (VOIs) were collected by point multiplication of these masks and the normalized T1 images. Radiomic features of the subcortical brain region were extracted by an in-house MATLAB script from each subject.[19,30]

Evaluation of White Matter Lesions

White matter hyperintensities (WMH) volume and Fazekas scale rating were used to evaluate WML. The volume of WMH was obtained from the T_1WI and T_2-FLAIR images. Three radiologists (W.Z., CM.L., and D.J.G., with 15, 20, and 28 years of experience in neuroimaging, respectively) who were blinded to the clinical information visually rated WML severity on T_2-FLAIR sequences by using the modified Fazekas scale.[31] The scoring criteria were as follows: 0 = absence, 1 = punctate foci, 2 = beginning confluence of foci, 3 = large confluent areas. After the review by each radiologist, the interobserver agreement was obtained. The consistency of the results was tested among the three radiologists.

Radiomics Model Building and Evaluation

Spearman rank correlation was used to calculate feature redundancy by calculating the correlation coefficient between features to remove the highly correlated features with correlation coefficient greater than 0.9, and univariate cox analysis was used to select the features with significant differences ($P < 0.05$). The least absolute shrinkage and selection operator (LASSO) Cox regression algorithm with 10-fold cross validation was used to select the features that were mostly relevant to the TTP. The radiomics score (rad-score) of each patient was calculated by a linear combination of the chosen features multiplied by their respective coefficients. The performance of the radiomics

TABLE 1. Baseline Characteristics of the MCI Patients in the Training Cohort and Testing Cohort

Variable	Training Cohort	Testing Cohort	Statistics	*P*-value
Fazekas scale				
0	6 (5.36%)	0 (0.00%)	-	0.115
1	87 (77.68%)	45 (90.00%)		
2	18 (16.07%)	4 (8.00%)		
3	1 (0.89%)	1 (2.00%)		
Sex				
Male	61 (54.46%)	35 (70.00%)	3.456	0.063
Female	51 (45.54%)	15 (30.00%)		
Alcohol abuse				
No	108 (96.43%)	49 (98.00%)	0.002	0.966
Yes	4 (3.57%)	1 (2.00%)		
APOE ε4 alleles				
No	58 (51.79%)	24 (48.00%)	0.198	0.656
Yes	54 (48.21%)	26 (52.00%)		
Age (years)	71.74 ± 7.34	72.05 ± 6.10	0.282	0.778
Education (years)	16.00 (14.00, 18.00)	16.00 (14.00, 18.00)	−0.743	0.457
BMI (kg/m^2)	27.18 (24.50, 30.07)	26.44 (24.76, 31.35)	0.098	0.922
MoCA	23.00 (21.00, 25.00)	23.50 (21.00, 25.00)	1.245	0.213
ADAS-Cog11	10.00 (7.00, 13.00)	9.00 (5.95, 11.05)	−1.679	0.093
ADAS-Cog13	16.00 (12.00, 21.00)	14.00 (10.95, 20.00)	−1.22	0.222
CDR	0.50 (0.50, 0.50)	0.50 (0.50, 0.50)	−0.203	0.839
FAQ	2.00 (0.00, 5.00)	2.00 (0.00, 6.00)	0.923	0.356
GDS	2.00 (1.00, 3.00)	1.00 (0.00, 3.00)	−0.983	0.326
MMSE	28.00 (27.00, 29.00)	28.00 (27.00, 29.00)	0.227	0.821
RAVLT immediate	34.00 (28.00, 41.00)	35.50 (26.00, 39.10)	−0.176	0.86
RAVLT learning	4.00 (2.00, 7.00)	4.00 (2.00, 6.00)	0.241	0.809
RAVLT forgetting	5.00 (4.00, 7.00)	5.00 (3.00, 6.05)	−0.803	0.422
RAVLT percent forgetting	66.67 (43.57, 100.00)	70.71 (33.33, 88.12)	−1.053	0.292
AFT	16.92 ± 4.50	18.04 ± 5.91	1.194	0.236
Aβ1-42 (pg/mL)	990.00 (740.75, 1377.20)	880.50 (675.90, 1483.85)	−0.702	0.483
Aβ1-40 (pg/mL)	8740.00 (6650.45, 10297.45)	8734.50 (7219.85, 9687.30)	−0.105	0.916
Aβ1-38 (pg/mL)	1964.50 (1553.90, 2401.60)	1992.50 (1686.85, 2289.05)	0.344	0.731
T-tau (pg/mL)	253.25 (202.35, 349.11)	281.95 (213.29, 400.60)	1.001	0.317
P-tau (pg/mL)	24.29 (17.65, 34.84)	26.27 (18.94, 39.67)	0.943	0.346
WMH Volume (cm^3)	4.57 (1.45, 13.08)	4.88 (2.28, 12.03)	0.558	0.577

MCI = mild cognitive impairment; BMI = body mass index; ADAS-Cog = Alzheimer's Disease Assessment Scale-Cognitive subscale; CDR = Clinical Dementia Rating; FAQ = Functional Assessment Questionnaire; GDS = Geriatric Depression Scale; MMSE = Mini–Mental State Examination; RAVLT = Rey Auditory Verbal Learning Test; AFT = Animal Fluency Test; Aβ = amyloid-β; T-tau = Total tau; P-tau = Phosphorylated tau; WMH = white matter hyperintensities.
A chi square test or Fisher's exact test was used for the nominal variable. A Mann–Whitney test was used for the continuous variable with abnormal distribution.

model was evaluated by the concordance index (C-index) in the training cohort and independently verified in the validation cohort.

Clinical-Laboratory Model Building and Evaluation

The potential predictors among the clinical, laboratory, and WML's parameters were identified by using a univariate Cox proportional hazards regression model in the training cohort. These factors ($P < 0.05$) from the univariate analysis were used to established clinical, laboratory, and clinical-laboratory models by multivariate Cox proportional hazard model. The models were independently verified in the validation dataset.

Combined Models Building and Evaluation

The potential predictors among the clinical, laboratory and WML's parameters were identified by using a univariate Cox proportional hazards regression model in the training cohort. Using the same features as the radiomics models and clinical-laboratory model, a multivariate Cox proportional hazard model was adopted to establish a radiomics-clinical model by the radiomics and clinical measures, and another was also created combining radiomics, clinical, and laboratory features in a model. The two combined models were independently validated in the validation dataset, and the performance was evaluated by C-index with a 95% confidence interval (95% CI). Patients were divided into high-risk group and low-risk group according to the median value in the radiomics-clinical-laboratory model to predict the risk of AD progression in the next 5 years. KM survival curve analyses were utilized to explore the potential associations between the radiomics-clinical-laboratory model and TTP. The log-rank tests were used for the comparisons of the KM analysis.

Multipredictor Nomogram Construction

A multipredictor nomogram, which incorporated clinical, laboratory and radiomics risk factors, was constructed based on the multivariate Cox analysis. The calibration of the multipredictor nomogram was assessed by calibration curves, which were used for the comparison of the consistency between the clinical results and the TTP predicted by the multipredictor nomogram.

Statistical Analysis

The R software (v. 3.6.0; http://www.Rproject.org) was used for the data analyses and all variables were expressed as the mean ± standard deviation (SD) or median (interquartile range [IQR]). The Shapiro–Wilk test and the Bartlett test were applied to test the distribution of the clinical, laboratory characteristics and image features. And then the Student's t-test, Mann–Whitney U-test, or the Chi-squared test were used to compare between-group differences base on the distributions. The discriminant performance of each model was quantified by C-index with 95%CI both in the training and in the validation dataset. The Akaike information criterion (AIC) was calculated to assess the risk of overfitting. The interobserver reproducibility was assessed with the intraclass correlation coefficient (ICC). A two tailed $P < 0.05$ was regarded statistically significant.

Results

Patients Characteristics

There was no significant difference ($P = 0.063$–0.966) in both the clinical and laboratory characteristics between the training group and validation group (Table 1). A total of 68 (68/162, 41.9%) patients progressed to AD within 5 years. The overall 1-, 3-, and 5-year cumulative progression rates were 16.6% (27/162), 34.5% (56/162), and 41.9% (68/162), respectively.

Radiomics Features Selection and Radiomics Signature Construction

Totally 4864 features (1198 features from the cortex and 3666 features from the subcortical region) were obtained from brain. First, Spearman correlation analysis was used to reduce the redundancy by calculating the correlation coefficient between features. A total of 2298 features remained after the highly correlated features with correlation coefficient greater than 0.9 were removed. Second, univariate cox analysis was used to select the features with significant differences ($P < 0.05$) and 325 features were remained. Third, the LASSO Cox regression algorithm with 10-fold cross validation was used to select the features that were mostly relevant to the TTP. After the above steps, totally 33 radiomics features were finally selected (Fig. 2), with 20 features belonging to morphology, 6 features were image intensity related, and 7 belonged to textural features. Totally 13 features were from the bilateral hippocampus and temporal cortex. The feature coefficients were shown in Fig. 2.

Selection of Clinical and Laboratory Characteristics

Table 2 showed the univariate analysis of the clinical and laboratory characteristics in the training dataset. The results indicated that the Montreal Cognitive Assessment (MoCA) (hazard ratio [HR], 0.798; 95% confidence interval [CI], 0.734–0.869), the Alzheimer's Disease Assessment Scale (ADAS, both 13 and 11 questionnaires), ADAS-Cog11 (HR, 1.257; 95% CI, 1.174–1.346), ADAS-Cog13 (HR, 1.162; 95% CI, 1.111–1.215), the Functional Activities Questionnaire (FAQ) (HR, 1.186; 95% CI, 1.133–1.241), the Mini-Mental State Examination (MMSE) (HR, 0.750; 95% CI, 0.647–0.869), the Rey Auditory-Verbal Learning Test (RAVLT), RAVLT immediate (HR, 0.915; 95% CI, 0.879–0.952), RAVLT learning (HR, 0.851; 95% CI, 0.758–0.954), RAVLT forgetting (HR, 1.123; 95% CI, 1.007–1.251), RAVLT percent forgetting (HR, 1.024; 95% CI, 1.012–1.036), the Animal Fluency Test (AFT) (HR, 0.894; 95% CI, 0.836–0.956), APOE ε4 (HR, 2.627; 95% CI, 1.435–4.811), Aβ 1–42 (HR, 0.998; 95% CI, 0.997–0.999), T-tau (HR, 1.004; 95% CI, 1.002–1.006), and P-tau (HR, 1.037; 95% CI, 1.022–1.053) were risk factors associated with the TTP from MCI to AD.
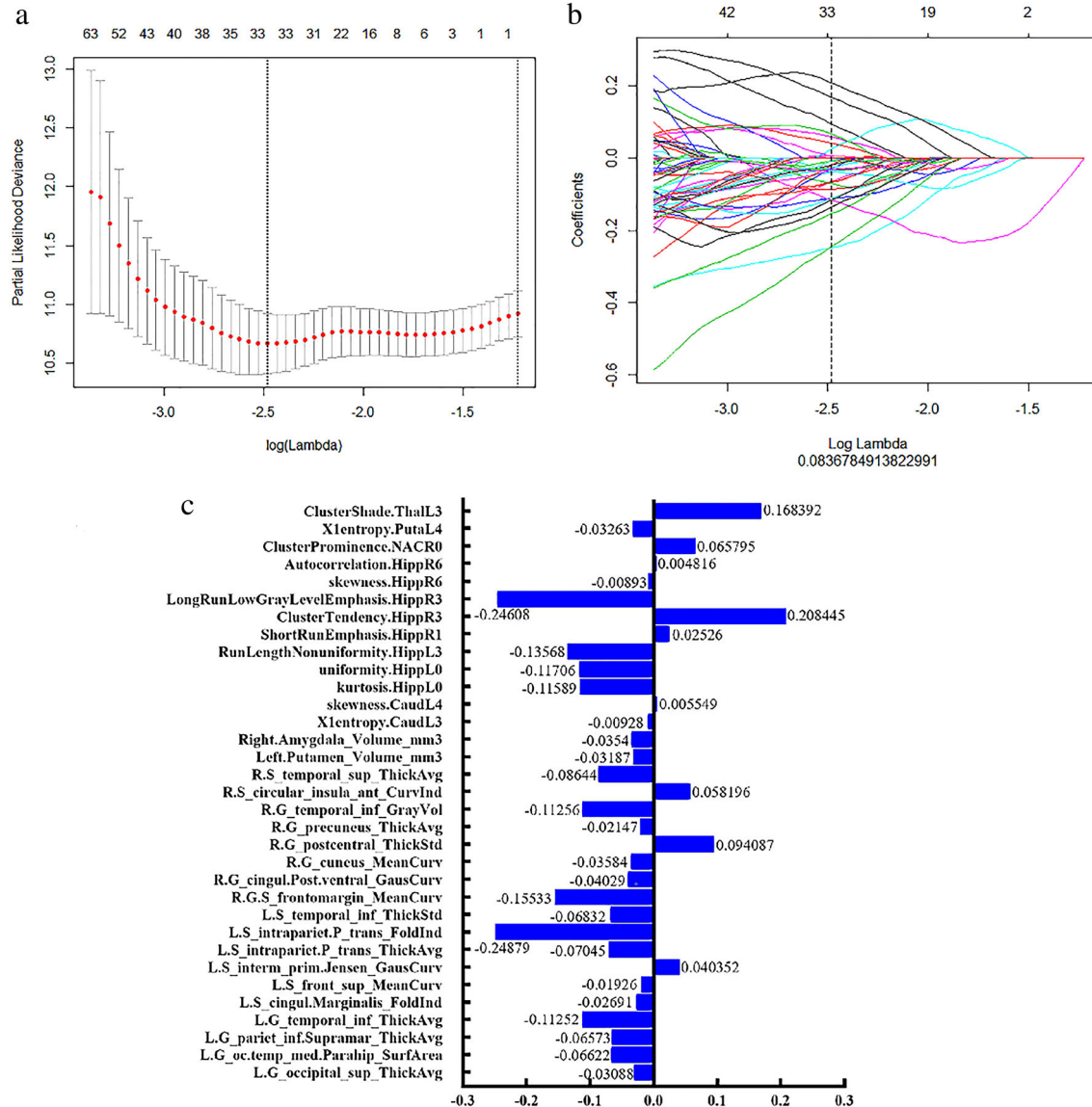
FIGURE 2: Radiomics feature selection using the LASSO Cox regression with a 10-fold crossvalidation. Tuning parameter selection in the LASSO Cox regression model (a). LASSO coefficient analysis of the radiomics features (b). Using 10-fold crossvalidation, 33 nonzero coefficients were selected (c).

Estimation of the Performance of Different Models and Verification

In the training cohort, the C-index of the models built with radiomics, clinical, laboratory, clinical-laboratory, radiomics-clinical and radiomics-clinical-laboratory features were 0.924 (95% CI: 0.894–0.952), 0.863 (95% CI: 0.812–0.913), 0.763 (95% CI: 0.690–0.835), 0.903 (95% CI: 0.868–0.938), 0.943 (95% CI: 0.921–0.964), and 0.950 (95% CI: 0.929–0.971). In the validation cohort, the C-index of the radiomics, clinical, laboratory, clinical-laboratory, radiomics-clinical and radiomics-clinical-laboratory models were 0.811 (95% CI: 0.707–0.914), 0.865 (95% CI: 0.775–0.955), 0.748 (95% CI: 0.650–0.846), 0.901 (95% CI: 0824–0.977), 0.881 (95% CI: 0.796–0.965) and 0.907 (95% CI: 0.836–0.979), respectively. Among these models, the radiomics-clinical-laboratory model showed the highest

performance ($P < 0.05$) (Table 3). KM survival curve analyses based on the radiomics-clinical-laboratory model was shown in Fig. 3. The cutoff value of the radiomics-clinical-laboratory model was −4.68986, which was regarded as the median value used for risk stratification. There were significant TTP differences between the low- and high-risk subgroups.

Multipredictor Nomogram Construction and Validation

A multipredictor nomogram based on the radiomics-clinical-laboratory model was made consisting of 15 predictors, including the MoCA, ADAS-Cog11, ADAS-Cog13, FAQ, MMSE, RAVLT immediate, RAVLT learning, RAVLT forgetting, RAVLT percent forgetting, APOE ε4, Aβ 1–42, T-tau, P-tau, and rad-score for the individualized estimation of the TTP (Fig. 4). The calibration curves indicated that the

TABLE 2. Factors Related to the Prediction of Conversion Time in the Training Cohort

Variables	Hazard Ratio	95% CI	P-value
Age (years)	0.9935	0.955–1.033	0.745
Sex (M/F)	1.21	0.683–2.145	0.513
Education (years)	0.956	0.861–1.061	0.397
Alcohol use	2.446	0.758–7.895	0.135
BMI (kg/m^2)	0.945	0.883–1.012	0.105
MOCA	0.798	0.734–0.869	<0.05*
ADAS-Cog.11	1.257	1.174–1.346	<0.05*
ADAS-Cog.13	1.162	1.111–1.215	<0.05*
CDR	NA	NA	NA
FAQ	1.186	1.133–1.241	<0.05*
GDS	1.078	0.92–1.264	0.352
MMSE	0.750	0.647–0.869	<0.05*
RAVLT immediate	0.915	0.879–0.952	<0.05*
RAVLT learning	0.851	0.758–0.954	<0.05*
RAVLT forgetting	1.123	1.007–1.251	<0.05*
RAVLT percent forgetting	1.024	1.012–1.036	<0.05*
AFT	0.894	0.836–0.956	<0.05*
APOE ε4 alleles	2.627	1.435–4.811	<0.05*
Aβ1-42 (pg/mL)	0.998	0.997–0.999	<0.05*
Aβ1-40 (pg/mL)	0.999	0.999–1	0.149
Aβ1-38 (pg/mL)	0.999	0.999–1	0.088
T-tau (pg/mL)	1.004	1.002–1.006	<0.05*
P-tau (pg/mL)	1.037	1.022–1.053	<0.05*
WMH Volume (cm^3)	1.002	0.974–1.03	0.908
Fazekas Scale	1.289	0.731–2.27	0.38

BMI = body mass index; ADAS-Cog = Alzheimer's Disease Assessment Scale-Cognitive subscale; CDR = Clinical Dementia Rating; FAQ = Functional Assessment Questionnaire; GDS = Geriatric Depression Scale; MMSE = Mini–Mental State Examination; RAVLT = Rey Auditory Verbal Learning Test; AFT = Animal Fluency Test; Aβ = amyloid-β; T-tau = total tau; P-tau = phosphorylated tau; WHM = white matter hyperintensities.
*P values less than 0.05 were identified statistically significant. Significant variables with $P < 0.05$ in the univariate analysis were considered as risk factors for TTP and included in the multivariate Cox analysis, and the HR value is the Cox regression coefficient.

clinical results were in good agreement with the 1, 3, 5-year TTP predicted by the multi-predictor nomogram (Fig. 4).

Discussion

Early prediction of when a patient with MCI will progress to AD has always been a difficult and challenging task for AD prevention and targeted treatment. This study is the first time to establish and verify a radiomics model, which extracted features from the whole brain microstructure and combined with clinical and laboratory characteristics to accurately predict the progression time of MCI patients in 5 years. In accordance with the radiomics, clinical and biological information of the baseline, six prediction models were constructed and compared. We found that these models all achieved good results in terms of TTP prediction. The

TABLE 3. Prediction Performance of the Models

Models	Training Set			Testing Set		
	C-index inininindex	Lower	Upper	C-index	Lower	Upper
Radiomics	0.924	0.894	0.952	0.811	0.707	0.914
Clinical	0.863	0.812	0.913	0.865	0.775	0.955
Laboratory	0.763	0.690	0.835	0.748	0.65	0.846
Clin-lab	0.903	0.868	0.938	0.901	0.824	0.977
Rad-clin	0.943	0.921	0.964	0.881	0.796	0.965
Rad-clin-lab	0.950	0.929	0.971	0.907	0.836	0.979

Clin-lab, Clinical-laboratory; Rad-clin, Radiomics-clinical; Rad-clin-lab, Radiomics-clinical-laboratory.
The performance of these models was evaluated by the C-index in the training cohort and independently verified in the validation cohort.
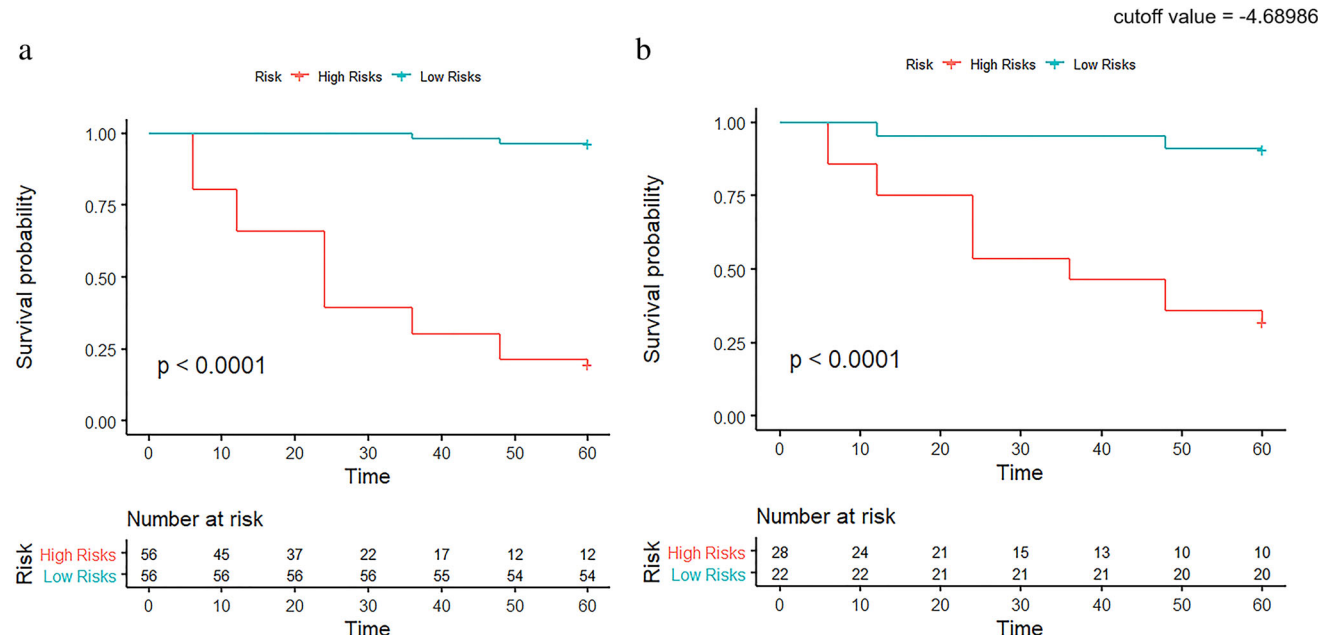
FIGURE 3: KM analyses of the TTP based on the radiomics-clinical-laboratory model with cutoff values as the median of the training cohort (a) and the validation cohort (b). There were significant differences between the low- and high-risk subgroups (log-rank test, P < 0.05, respectively).

radiomics model showed strong prognostic capability. After adding clinical and laboratory features, the prediction accuracy was further improved. The prognostic model established by the combination of radiomics, laboratory and clinical measures showed the best performance compared with other models ($P < 0.05$). We provided a direct calculation method for clinicians to estimate the possibility of progression of MCI patients in a specific time frame. This method is simple, noninvasive, and without the disadvantages of radiation used in Positron emission computed tomography (PET) imaging. Previously, many studies on the prediction of the MCI progression to AD solely focused on the imaging characteristics of the hippocampus and temporal cortex.[10–12,32] For example, a deep learning method based on hippocampal MRI has been developed, with a C-index of 0.864.[9] In another study, a 3-year conversion rate was predicted based on the thickness of the middle temporal cortex, hippocampal volume and some psychological scales, with a c-index of 0.78.[10] In comparison with the literature, our results provided higher accuracy. Our study included the whole cerebral cortex, white matter and subcortical nucleus, comprehensively analyzing a large number of microstructural features, including morphological features, signal intensity features, texture features and high-order features, and verified the results using independent
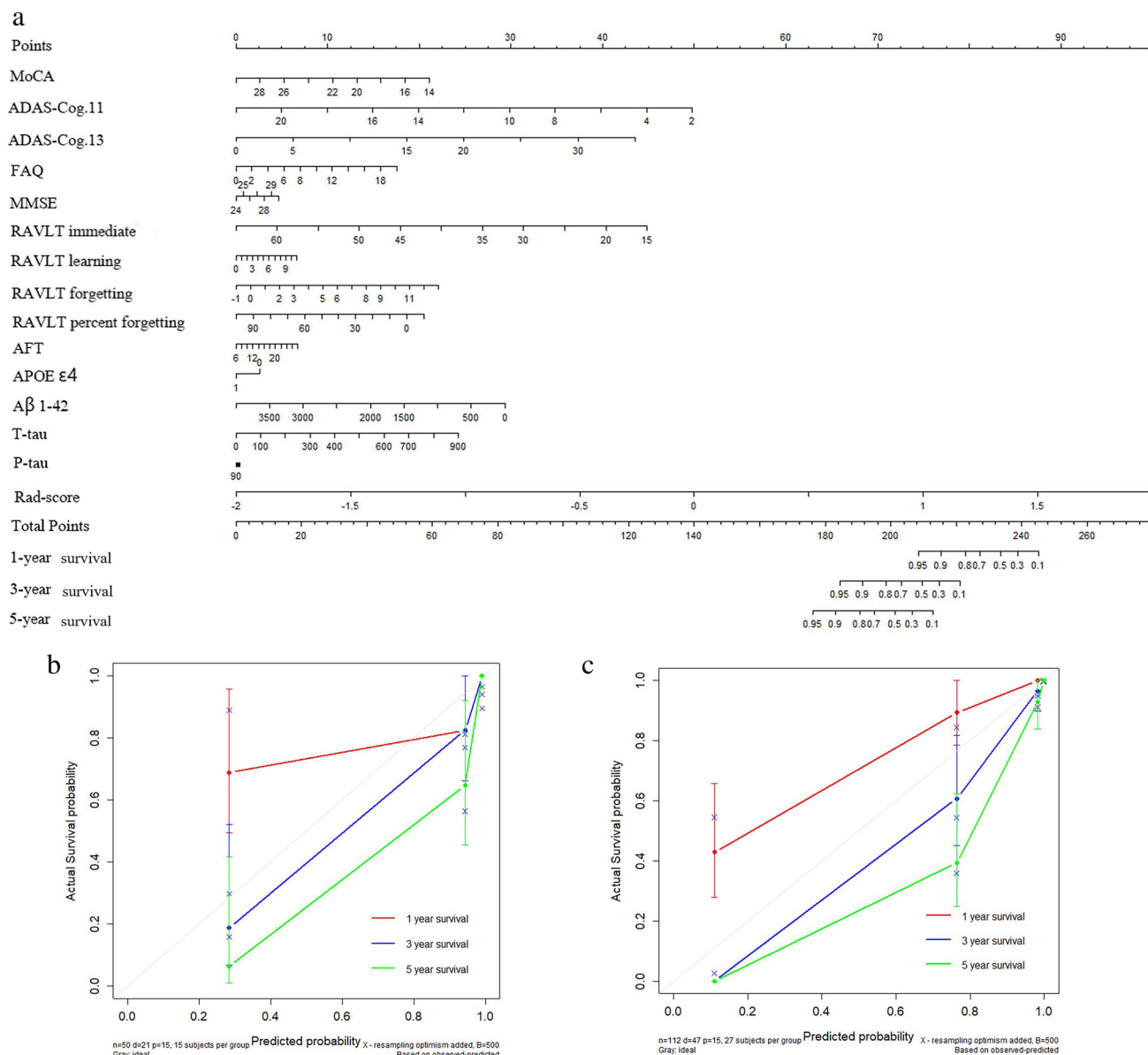
FIGURE 4: The multi-predictor nomogram (a) was used to estimate the TTP of MCI subjects individually, along with the assessment of the model calibration. Calibration plot for the multi-predictor nomogram to the 1-, 3-, 5-year TTP in the training dataset (b) and the validation dataset (c). The diagonal line indicates the ideal value, and the solid line represents the performance of the nomogram; the closer the solid line is to the diagonal dashed line, the better the calibration will be.

verification set. On the other hand, the duration of follow-up is important to identify very early markers and to reduce false negative cases. Previous studies mostly underlined a short-term follow-up of 1 to 3 years.[24–26] In this study, however, all MCI subjects were followed up for 5 years.

In the current study, 33 radiomic features of morphological, intensity, and texture associated with the TTP of MCI were identified. The intensity and texture features could reflect the texture heterogeneity of different brain structures. The heterogeneity may originate from the brain microscopic changes such as Aβ plaques deposition and neurofibrillary tangles (NFTs), which has strong ability to evaluate the

clinical prognosis. The accumulation of NFTs and Aβ plaques indicates the early pathological change of AD, which appears earlier than brain atrophy.[17] The 33 radiomic features were mostly located in the temporal cortex, hippocampus, and subcortical nuclei. The temporal cortex[33] and hippocampus[34] are the main brain regions responsible for memory, and the changes of their function and structure could occur in the early stage of AD.[6,27,33,35] The function of subcortical nuclei are related to motor, emotion, motivation, association, and cognition.[36] Previously, reports have revealed that the reduced volume of putamen and amygdala were independently associated with cognitive impairment.[13,14] Therefore,

the changes of the structure of hippocampus, cortex and sub-cortical nuclei are the signs of the upcoming transformation of MCI, which could be taken into consideration to predict the progression in advance.

In addition to the radiomic features, the clinical and laboratory information were also essential, that they could significantly improve the performance of early prediction of AD. In clinical aspect, the MoCA, ADAS-Cog11, ADAS-Cog13, FAQ, MMSE and RAVLT were finally included in the best model.[9,28,37] All of these features are common cognitive scales in nervous system research and are adopted to evaluate cognitive ability of memory, attention, and executive function. In terms of laboratory indicators, the biomarkers of APOE ε4, Aβ 1–42 and tau protein were risk factors associated with the TTP of MCI. The APOE ε4 is the most common susceptible gene for AD.[38] Previous studies have reported that APOE ε4 has predictive value for the transformation of MCI to AD.[10,11] Aβ and tau proteins are the key neuropathological factors in the pathogenesis of AD, with misfolding and accumulation leading to progressive neuronal loss.[39] In this study, we found that only Aβ 1–42, among the three subtypes of Aβ, has a significant correlation with TTP. The possible reason is that Aβ 1–42 is more likely to accumulate than the other two subtypes during the progression of MCI.[40]

In this study, a visual multipredictor nomogram was developed from the radiomics-clinical-laboratory model. This multipredictor nomogram could estimate the 1-, 3-, and 5-year risk of MCI conversion for each subject, which would be of great assistance for the clinicians to carry out individualized prediction and early intervention. From the calibration curve, the 1-, 3-, 5-year TTP estimation demonstrates good consistency with the actual clinical results. In addition, the median value of the model provided a good measure to divide patients into high- and low-risk subgroups. It could provide important value for clinical early detection and timely treatment by stratified MCI subjects and finding high-risk groups who are more likely to develop to AD.

Limitations

First, due to our strict inclusion criteria for 5 year following up, the sample size was relatively small. Second, this study only focused on the baseline data of MCI subjects, and did not analyze the dynamic follow-up data. Third, this study focused on the early detection of AD transformation from MCI and did not pay attention to the earlier stage before MCI, such as subjective cognitive impairment (SCD) and normal people. In the future, larger samples with an external validation should be considered to track and analyze the dynamic data of MCI, normal people and patients with SCD for further enhancing the timeliness and reliability of the prediction.

Conclusion

This study developed a time-to-event model, including the radiomic characteristics obtained from MRI imaging, the clinical information and the laboratory measurements, and established a multipredictor nomogram to accurately estimate the time and risk of a single MCI converting to AD with high accuracy. MCI subjects could be stratified into subgroups and high-risk individuals could be screened out and treated timely to delay the progression of AD.

References

1. Alzheimer's A. 2016 Alzheimer's disease facts and figures. Alzheimers Dement 2016;12(4):459-509..

2. Zhang C, Kong M, Wei H, et al. The effect of ApoE epsilon 4 on clinical and structural MRI markers in prodromal Alzheimer's disease. Quant Imaging Med Surg 2020;10(2):464-474.

3. Mueller SG, Weiner MW, Thal LJ, et al. Ways toward an early diagnosis in Alzheimer's disease: The Alzheimer's disease neuroimaging initiative (ADNI). Alzheimers Dement 2005;1(1):55-66.

4. Dubois B, Hampel H, Feldman HH, et al. Preclinical Alzheimer's disease: Definition, natural history, and diagnostic criteria. Alzheimers Dement 2016;12(3):292-323.

5. Knodel J. The diagnosis and management of mild cognitive impairment: A clinical review. JAMA 2014;312(23):2551-2561.

6. Querbes O, Aubry F, Pariente J, et al. Early diagnosis of Alzheimer's disease using cortical thickness: Impact of cognitive reserve. Brain 2009;132(Pt 8):2036-2047.

7. Querbes O, Lotterie JA, Pariente J, et al. IC-P2-126: MRI-based cortical thickness measurement improves the prediction of MCI to AD conversion. Alzhmers Dementia 2008;4(4-supp-S):T57-T57.

8. Vos S, van Rossum I, Burns L, et al. Test sequence of CSF and MRI biomarkers for prediction of AD in subjects with MCI. Neurobiol Aging 2012;33(10):2272-2281.

9. Li H, Habes M, Wolk DA, et al. A deep learning model for early prediction of Alzheimer's disease dementia based on hippocampal magnetic resonance imaging data. Alzheimers Dement 2019;15(8):1059-1070.

10. Barnes DE, Cenzer IS, Yaffe K, Ritchie CS, Lee SJ. Alzheimer's disease neuroimaging I. a point-based tool to predict conversion from mild cognitive impairment to probable Alzheimer's disease. Alzheimers Dement 2014;10(6):646-655.

11. Dickerson BC, Wolk DA. Alzheimer's disease neuroimaging I Biomarker-Based Prediction of Progression in MCI: Comparison of AD Signature and Hippocampal Volume with Spinal Fluid Amyloid-Beta and Tau. Front Aging Neurosci 2013;5:55.

12. Li K, O'Brien R, Lutz M, Luo S. Alzheimer's disease neuroimaging I. a prognostic model of Alzheimer's disease relying on multiple longitudinal measures and time-to-event data. Alzheimers Dement 2018;14(5):644-651.

13. de Jong LW, van der Hiele K, Veer IM, et al. Strongly reduced volumes of putamen and thalamus in Alzheimer's disease: An MRI study. Brain 2008;131(Pt 12):3277-3285.

14. Horinek D, Varjassyova A, Hort J. Magnetic resonance analysis of amygdalar volume in Alzheimer's disease. Curr Opin Psychiatry 2007;20(3):273-277.

15. Teipel SJ, Born C, Ewers M, et al. Multivariate deformation-based analysis of brain atrophy to predict Alzheimer's disease in mild cognitive impairment. Neuroimage 2007;38(1):13-24.

16. Prins ND, van Dijk EJ, den Heijer T, et al. Cerebral white matter lesions and the risk of dementia. Arch Neurol 2004;61(10):1531-1534.

17. Sorensen L, Igel C, Liv Hansen N, et al. Early detection of Alzheimer's disease using MRI hippocampal texture. Hum Brain Mapp 2016;37(3):1148-1161.

18. Gillies RJ, Kinahan PE, Hricak H. Radiomics: Images are more than pictures they are data. Radiology 2016;278(2):563-577.

19. Aerts HJ, Velazquez ER, Leijenaar RT, et al. Decoding tumour phenotype by noninvasive imaging using a quantitative radiomics approach. Nat Commun 2014;5:4006.

20. Chaddad A, Desrosiers C, Hassan L, Tanougast C. Hippocampus and amygdala radiomic biomarkers for the study of autism spectrum disorder. BMC Neurosci 2017;18(1):52.

21. Shu ZY, Cui SJ, Wu X, et al. Predicting the progression of Parkinson's disease using conventional MRI and machine learning: An application of radiomic biomarkers in whole-brain white matter. Magn Reson Med 2021;85(3):1611-1624.

22. Belleville S, Fouquet C, Hudon C, Zomahoun HTV, Croteau J. Consortium for the early identification of Alzheimer's d-Q. neuropsychological measures that predict progression from mild cognitive impairment to Alzheimer's type dementia in older adults: A systematic review and meta-analysis. Neuropsychol Rev 2017;27(4):328-353.

23. Li S, Okonkwo O, Albert M, Wang MC. Variation in variables that predict progression from MCI to AD dementia over duration of follow-up. Am J Alzheimers Dis (Columbia) 2013;2(1):12-28.

24. Ahmed S, Mitchell J, Arnold R, Nestor PJ, Hodges JR. Predicting rapid clinical progression in amnestic mild cognitive impairment. Dement Geriatr Cogn Disord 2008;25(2):170-177.

25. Cui Y, Liu B, Luo S, et al. Identification of conversion from mild cognitive impairment to Alzheimer's disease using multivariate predictors. PLoS One 2011;6(7):e21896.

26. Landau SM, Harvey D, Madison CM, et al. Comparing predictors of conversion and decline in mild cognitive impairment. Neurology 2010;75(3):230-238.

27. Devanand DP, Pradhaban G, Liu X, et al. Hippocampal and entorhinal atrophy in mild cognitive impairment: Prediction of Alzheimer disease. Neurology 2007;68(11):828-836.

28. Hou XH, Feng L, Zhang C, Cao XP, Tan L, Yu JT. Models for predicting risk of dementia: A systematic review. J Neurol Neurosurg Psychiatry 2019;90(4):373-379.

29. Destrieux C, Fischl B, Dale A, Halgren E. Automatic parcellation of human cortical gyri and sulci using standard anatomical nomenclature. Neuroimage 2010;53(1):1-15.

30. Huynh E, Coroller TP, Narayan V, et al. CT-based radiomic analysis of stereotactic body radiation therapy patients with lung cancer. Radiother Oncol 2016;120(2):258-266.

31. Fazekas F, Chawluk JB, Alavi A, Hurtig HI, Zimmerman RA. MR signal abnormalities at 1.5 T in Alzheimer's dementia and normal aging. AJR Am J Roentgenol 1987;149(2):351-356.

32. Feng F, Wang P, Zhao K. Radiomic features of hippocampal subregions in alzheimer's disease and amnestic mild cognitive impairment. Front Aging Neurosci 2018;10:290.

33. Jack CR Jr, Petersen RC, Xu Y, et al. Rate of medial temporal lobe atrophy in typical aging and Alzheimer's disease. Neurology 1998;51(4):993-999.

34. Bird CM, Burgess N. The hippocampus and memory: Insights from spatial processing. Nat Rev Neurosci 2008;9(3):182-194.

35. West MJ, Coleman PD, Flood DG, Troncoso JC. Differences in the pattern of hippocampal neuronal loss in normal ageing and Alzheimer's disease. Lancet 1994;344(8925):769-772.

36. Herrero MT, Barcia C, Navarro JM. Functional anatomy of thalamus and basal ganglia. Childs Nerv Syst 2002;18(8):386-404.

37. Huang K, Lin Y, Yang L, et al. A multipredictor model to predict the conversion of mild cognitive impairment to Alzheimer's disease by using a predictive nomogram. Neuropsychopharmacology 2020;45(2):358-366.

38. Corder EH, Saunders AM, Strittmatter WJ, et al. Gene dose of apolipoprotein E type 4 allele and the risk of Alzheimer's disease in late onset families. Science 1993;261(5123):921-923.

39. Braak H, Braak E. Neuropathological stageing of Alzheimer-related changes. Acta Neuropathol 1991;82(4):239-259.

40. Goldberg TE. P4-065: Utility of combinations of biomarkers, cognitive markers, and risk factors to predict conversion from MCI to AD and magnitude of functional decline in ADNI subjects. Alzheimers Dement 2010;6(4):e40-e41.